

Form Factors of the Nucleon Axial and Pseudoscalar Currents

Chen Chen

University of Giessen

**Mass in the Standard Model and
Consequences of its Emergence**

April 19-24, 2021 on ZOOM Platform

Non-Perturbative QCD:

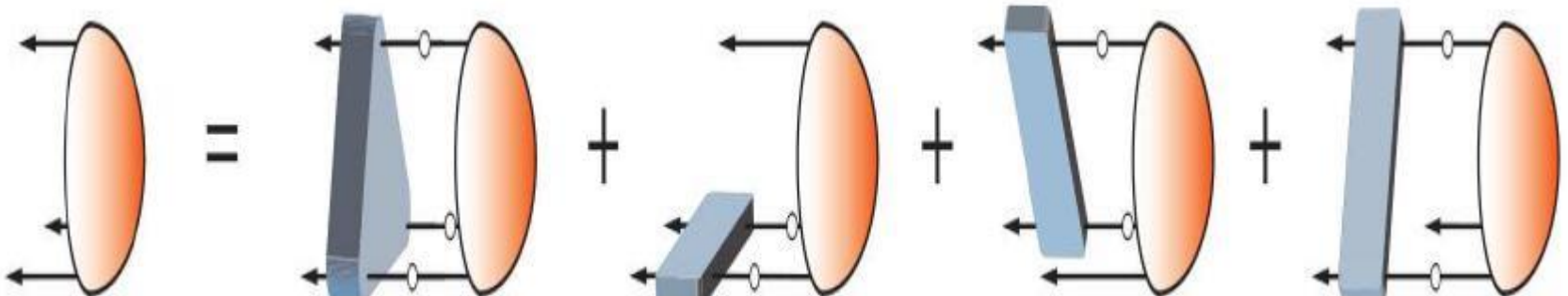
- Hadrons, as bound states, are dominated by non-perturbative QCD dynamics – Two emergent phenomena
 - **Confinement**: Colored particles have never been seen isolated
 - Explain how quarks and gluons bind together
 - **DCSB**: Hadrons do not follow the chiral symmetry pattern
 - Explain the most important mass generating mechanism for visible matter in the Universe
 - Neither of these phenomena is apparent in QCD's Lagrangian, HOWEVER, They play a dominant role in determining the characteristics of real-world QCD!

Non-Perturbative QCD:

- **From a quantum field theoretical point of view**, these emergent phenomena could be associated with dramatic, dynamically driven changes in the analytic structure of QCD's Schwinger functions (propagators and vertices). The Schwinger functions are solutions of the quantum equations of motion (**Dyson-Schwinger equations**).
- **The Gap equation of the dressed-quark propagator:**



- **Baryons: Faddeev equation**

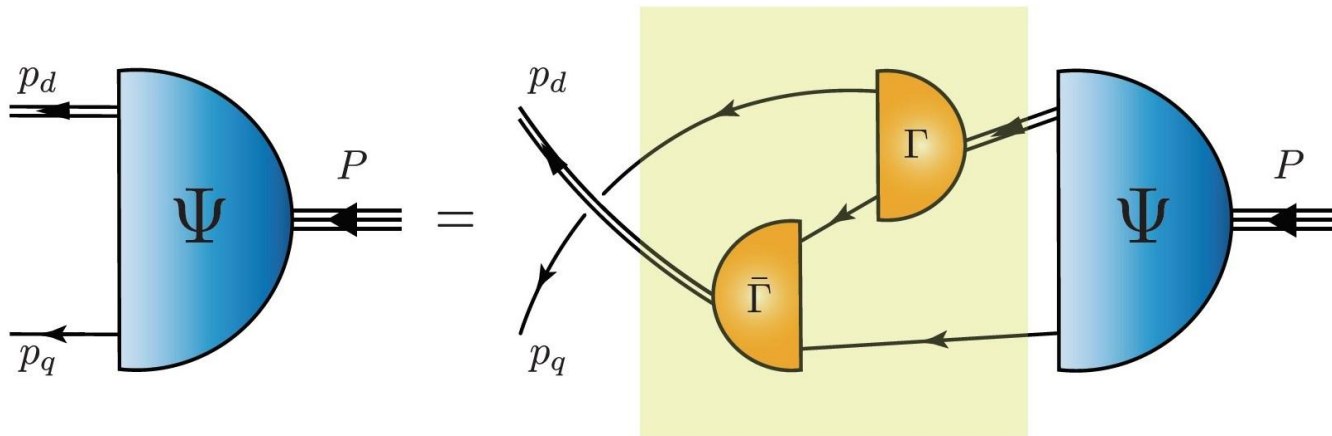


Non-Perturbative QCD:

- From a quantum field theoretical point of view, these emergent phenomena could be associated with dramatic, dynamically driven changes in the analytic structure of QCD's Schwinger functions (propagators and vertices). The Schwinger functions are solutions of the quantum equations of motion (**Dyson-Schwinger equations**).
- The Gap equation of the dressed-quark propagator:

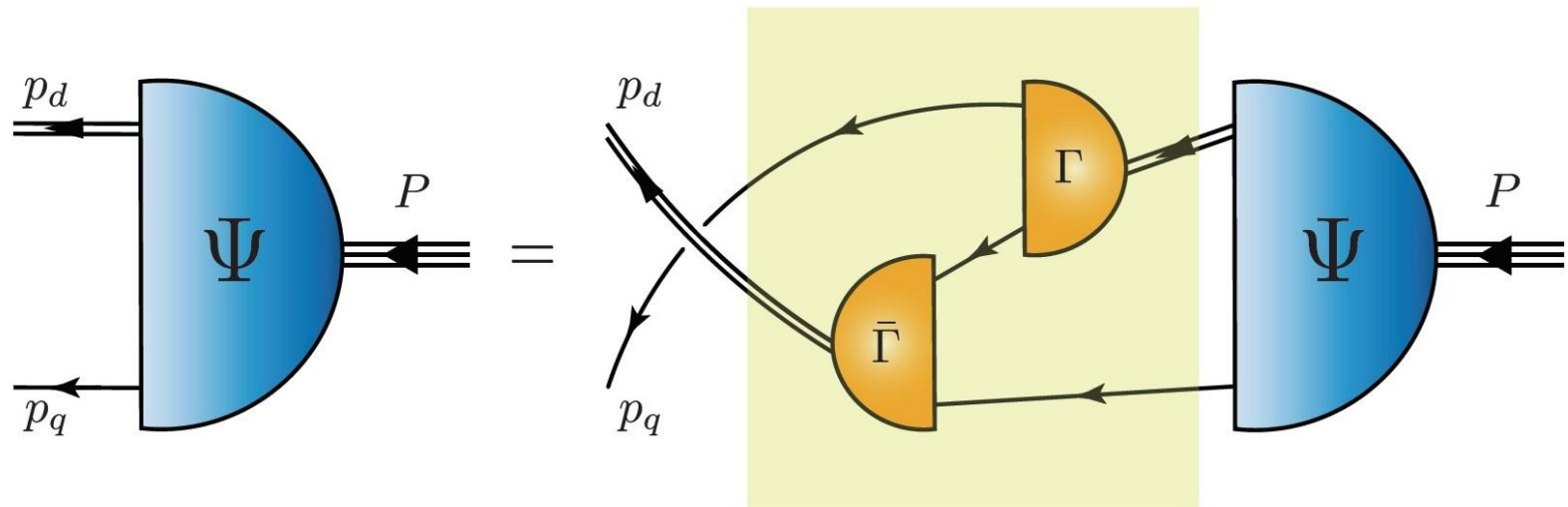


- Baryons: Faddeev equation



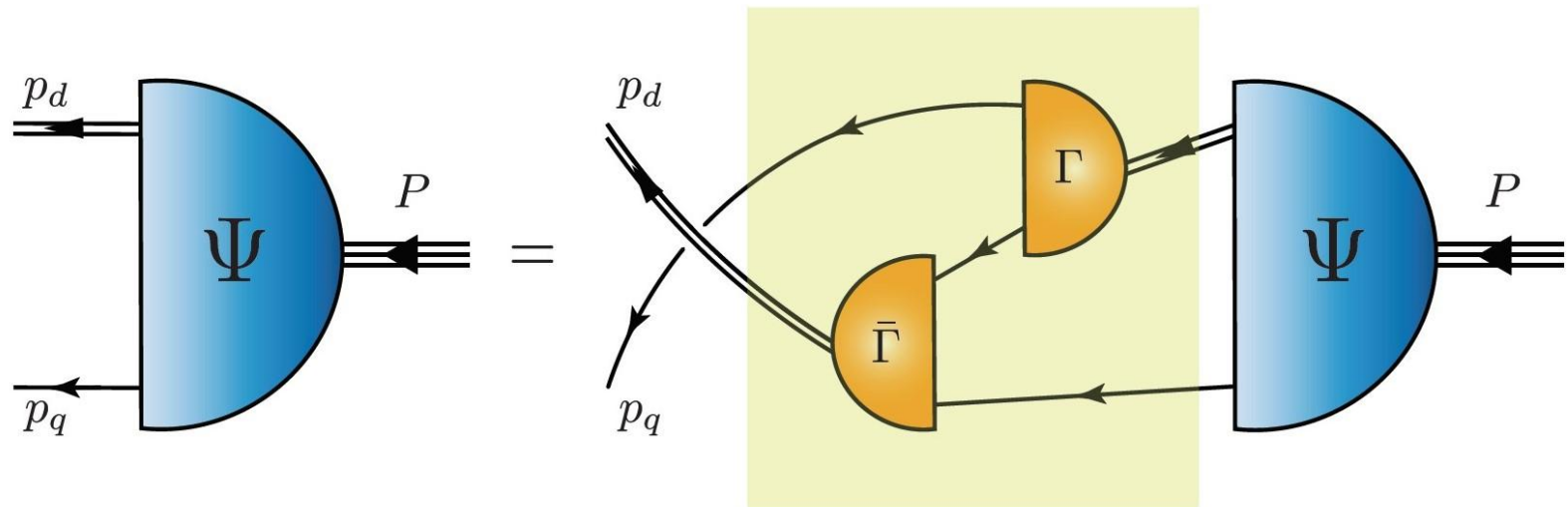
How to solve?

- ◆ The dressed-quark propagators
- ◆ Diquark amplitudes
- ◆ Diquark propagators
- ◆ **Faddeev amplitudes**



QCD-kindred model

- ◆ The dressed-quark propagators
- ◆ Diquark amplitudes
- ◆ Diquark propagators
- ◆ **Faddeev amplitudes**



QCD-kindred quark-diquark model

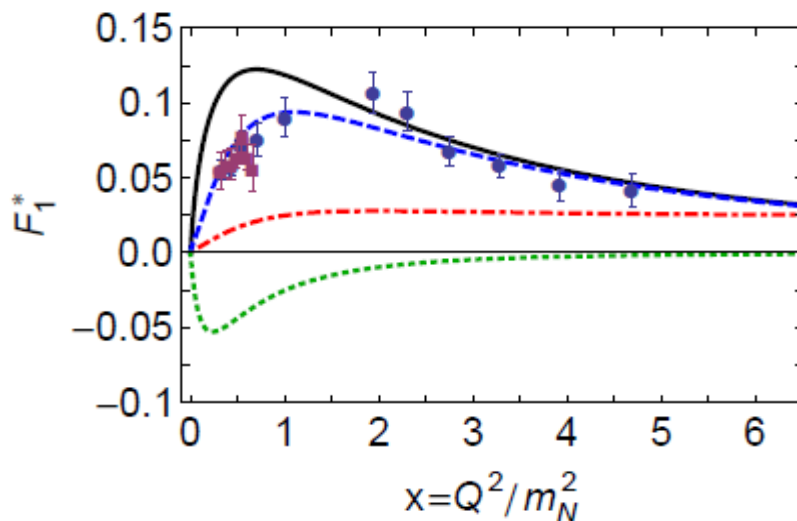
- **Parameters:** diquark masses
- These values provide for a good description of numerous dynamical properties of the nucleon, Δ -baryon and Roper resonance.
- **Solution to the 50 year puzzle -- Roper resonance:** Discovered in 1963, the Roper resonance appears to be an exact copy of the proton except that its mass is **50%** greater and it is unstable.

PRL 115, 171801 (2015)

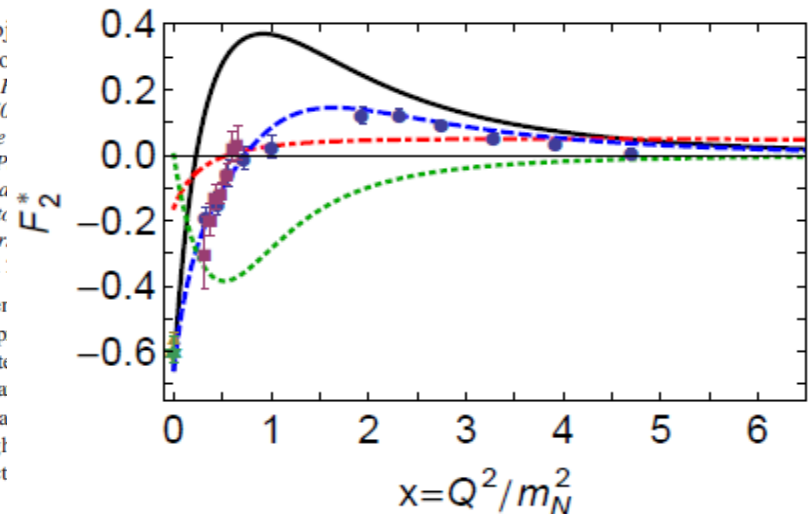
PHYSICAL REVIEW LETTERS

week ending
23 OCTOBER 2015

Completing the Picture of the Roper Resonance



Eduardo Roj
Xu,⁶ and He
ersitario de I
manca, E-376
Universidade
le Estadual P
Antioquia, Ca
onal Laborato
njing Univer.
ript received
ie three valer
erties of the p
alysis indicat
e dressed qua
he proton ana
mass by rough
electroproduct



DOI: 10.1103/PhysRevLett.115.171801

PACS numbers: 13.40.Gp, 14.20.Dh, 14.20.Gk, 11.15.Tk

Form Factors

- Form factors: contain important information about the structure and the properties of hadrons.
- Different probes correspond to different form factors.
- The nucleon electromagnetic current: electromagnetic form factors

$$J_{\mu}^{\text{EM}}(K, Q) = \bar{u}(P_f) \left[\gamma_{\mu} F_1(Q^2) + \frac{1}{2m_N} \sigma_{\mu\nu} Q_{\nu} F_2(Q^2) \right] u(P_i)$$

- A large number of experimental measurements, with high precision and up to large momentum transfer.

- The nucleon axial-vector current: axial-vector form factors

$$J_{5\mu}^j(K, Q) = \bar{u}(P_f) \frac{\tau^j}{2} \gamma_5 \left[\gamma_{\mu} G_A(Q^2) + i \frac{Q_{\mu}}{2m_N} G_P(Q^2) \right] u(P_i)$$

- The measurements are much more difficult, since they are related to weak processes.
- G_A – axial form factor: experimental data are rather sparse and with large uncertainties.
- G_P – induced pseudoscalar form factor: ONLY 4 empirical results.

- The nucleon pseudoscalar current: pseudoscalar form factor

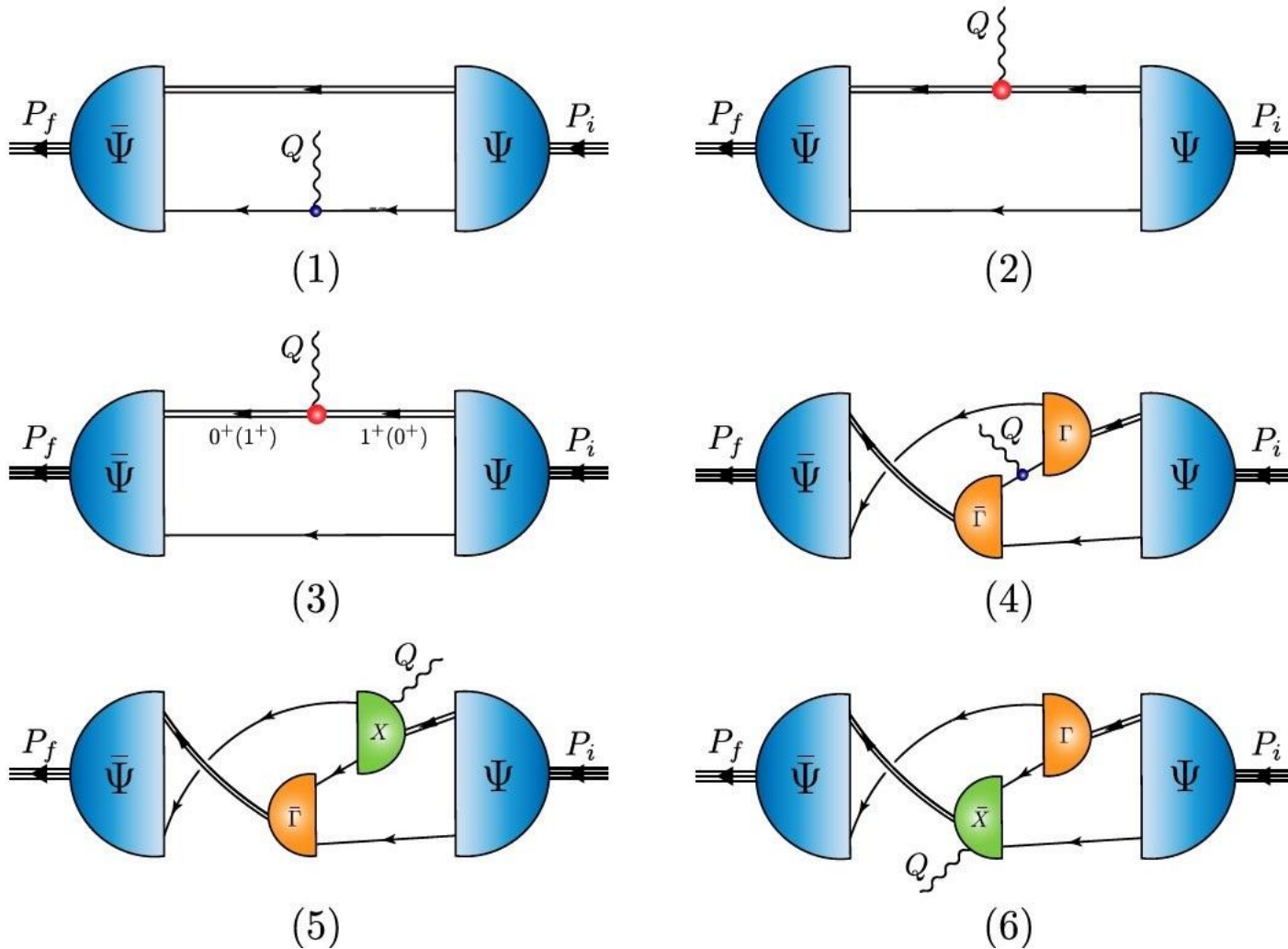
$$J_5^j(K, Q) = \bar{u}(P_f) \frac{\tau^j}{2} \gamma_5 G_5(Q^2) u(P_i)$$

- The Partially Conservation of the Axial Current (PCAC) relation:

$$G_A(Q^2) - \frac{Q^2}{4m_N^2} G_P(Q^2) = \frac{m_q}{m_N} G_5(Q^2)$$

How to compute Form Factors?

- In the quark-diquark framework, the associated symmetry-preserving current:



Electromagnetic Form Factors

- Hellstern, G. and Alkofer, Reinhard and Oettel, M. and Reinhardt, H., *Nucl.Phys.A* 627 (1997) 679-709.
- Bloch, Jacques C. R. and Roberts, Craig D. and Schmidt, S. M. and Bender, A. and Frank, M. R, *Phys.Rev.C* 60 (1999) 062201.
- Bloch, Jacques C. R. and Roberts, Craig D. and Schmidt, S. M., *Phys.Rev.C* 61 (2000) 065207.
- Oettel, Martin and Pichowsky, Mike and von Smekal, Lorenz, *Eur.Phys.J.A* 8 (2000) 251-281.
- Oettel, M. and Alkofer, Reinhard, *Phys.Lett.B* 484 (2000) 243-250.
- Oettel, M. and Alkofer, Reinhard and von Smekal, L., *Eur.Phys.J.A* 8 (2000) 553-566.
- Hecht, M. B. and Oettel, Martin and Roberts, C. D. and Schmidt, Sebastian M. and Tandy, Peter Charles and Thomas, Anthony William, *Phys.Rev.C* 65 (2002) 055204.
- Oettel, M. and Alkofer, Reinhard, *Eur.Phys.J.A* 16 (2003) 95-109.
- Alkofer, Reinhard and Holl, A. and Kloker, M. and Krassnigg, A. and Roberts, C. D., *Few Body Syst.* 37 (2005) 1-31.
- Nicmorus, Diana and Eichmann, Gernot and Alkofer, Reinhard, *Phys.Rev.D* 82 (2010) 114017.
- Eichmann, G. and Nicmorus, D., *Phys.Rev.D* 85 (2012) 093004.
- Segovia, Jorge and Cloet, Ian C. and Roberts, Craig D. and Schmidt, Sebastian M., *Few Body Syst.* 55 (2014) 1185-1222.
- Segovia, Jorge and El-Bennich, Bruno and Rojas, Eduardo and Cloet, Ian C. and Roberts, Craig D. and Xu, Shu-Sheng and Zong, Hong-Shi, *Phys.Rev.Lett.* 115 (2015) 17, 171801.
- Segovia, Jorge and Roberts, Craig D. and Schmidt, Sebastian M., *Phys.Lett.B* 750 (2015) 100-106
- Segovia, Jorge and Roberts, Craig D., *Phys.Rev.C* 94 (2016) 4, 042201.
- Chen, Chen and Lu, Ya and Binosi, Daniele and Roberts, Craig D. and Rodriguez-Quintero, Jose and Segovia, Jorge, *Phys.Rev.D* 99 (2019) 3, 034013.
- Lu, Ya and Chen, Chen and Cui, Zhu-Fang and Roberts, Craig D and Schmidt, Sebastian M and Segovia, Jorge and Zong, Hong Shi, *Phys.Rev.D* 100 (2019) 3, 034001.
- Cui, Zhu-Fang and Chen, Chen and Binosi, Daniele and de Soto, Feliciano and Roberts, Craig D and Rodriguez-Quintero, Jose and Schmidt, Sebastian M and Segovia, Jorge, *Phys.Rev.D* 102 (2020) 1, 014043.
- Eichmann, Gernot, *Phys.Rev.D* 84 (2011) 014014.
- Sanchis-Alepuz, Helios and Williams, Richard and Alkofer, Reinhard, *Phys.Rev.D* 87 (2013) 9, 096015.
- Sanchis-Alepuz, Helios and Fischer, Christian S., *Eur.Phys.J.A* 52 (2016) 2, 34.
- Sanchis-Alepuz, Helios and Alkofer, Reinhard and Fischer, Christian S., *Eur.Phys.J.A* 54 (2018) 3, 41.

Axial Form Factors

- Hellstern, G. and Alkofer, Reinhard and Oettel, M. and Reinhardt, H., *Nucl.Phys.A* 627 (1997) 679-709.
- Bloch, Jacques C. R. and Roberts, Craig D. and Schmidt, S. M., *Phys.Rev.C* 61 (2000) 065207.
- Oettel, Martin and Pichowsky, Mike and von Smekal, Lorenz, *Eur.Phys.J.A* 8 (2000) 251-281.

Axial Form Factors

- Hellstern, G. and Alkofer, Reinhard and Oettel, M. and Reinhardt, H., *Nucl.Phys.A* 627 (1997) 679-709.
- Bloch, Jacques C. R. and Roberts, Craig D. and Schmidt, S. M., *Phys.Rev.C* 61 (2000) 065207.
- Oettel, Martin and Pichowsky, Mike and von Smekal, Lorenz, *Eur.Phys.J.A* 8 (2000) 251-281.
- Eichmann, G. and Fischer, C. S., *Eur.Phys.J.A* 48 (2012) 9.

Nucleon axial and pseudoscalar form factors from the covariant Faddeev equation

Gernot Eichmann and Christian S. Fischer

Institut für Theoretische Physik, Justus-Liebig-Universität Giessen, D-35392 Giessen, Germany
(Dated: November 2, 2018)

We compute the axial and pseudoscalar form factors of the nucleon in the Dyson-Schwinger approach. To this end, we solve a covariant three-body Faddeev equation for the nucleon wave function and determine the matrix elements of the axialvector and pseudoscalar isotriplet currents. Our only input is a well-established and phenomenologically successful ansatz for the nonperturbative quark-gluon interaction. As a consequence of the axial Ward-Takahashi identity that is respected at the quark level, the Goldberger-Treiman relation is reproduced for all current-quark masses. We discuss the timelike pole structure of the quark-antiquark vertices that enters the nucleon matrix elements and determines the momentum dependence of the form factors. Our result for the axial charge underestimates the experimental value by 20–25% which might be a signal of missing pion-cloud contributions. The axial and pseudoscalar form factors agree with phenomenological and lattice data in the momentum range above $Q^2 \sim 1 \dots 2 \text{ GeV}^2$.

PACS numbers: 11.80.Jy 12.38.Lg, 11.40.Ha 14.20.Dh

I. INTRODUCTION

The nucleon's axial and pseudoscalar form factors are of fundamental significance for the properties of the nucleon that are probed in weak interaction processes. Their momentum dependence can be experimentally tested by (anti)neutrino scattering off nucleons or nuclei, charged pion electroproduction and muon capture processes; see [1–3] for reviews. Both form factors are experimentally hard to extract and therefore considerably less well known than their electromagnetic counterparts. Precisely measured is only the low-momentum limit g_A of the axial form factor which is determined from neutron β -decay. Planned experiments at major facilities are expected to change this situation in the near future.

The theoretical calculation of the nucleon's axial and pseudoscalar form factors requires genuinely non-perturbative methods. Chiral perturbation theory has been successful in this respect [1, 4, 5] although it is generally limited to the region of low momentum transfer. Recent studies in lattice gauge theory are getting closer to the physical pion mass region [6–8] but finite-volume effects become increasingly important. Another non-perturbative approach is the one via functional meth-

The study of axial and pseudoscalar form factors in the functional approach has so far been limited to an approximation where the nucleon is treated as a bound object of a quark and a diquark that interact via quark exchange [12, 13]. The entire gluonic substructure appears here only implicitly within the dressing of quark and diquark propagators as well as diquark vertex functions. There are several conceptual issues that complicate the treatment of form factors in the quark-diquark model. First, the requirement of current conservation induces the appearance of intricate 'seagull' diagrams [14]. Such terms have been taken into account for electromagnetic form factors, but their implementation in the case of axial form factors has not yet been possible for technical reasons [13]. Second, to comply with chiral Ward identities, a current-conserving quark-diquark model requires vector diquarks in addition to the usual scalar and axialvector diquark degrees of freedom [15]. Such an elaborate treatment of the quark-diquark model has not yet been performed.

The situation is somewhat different when the nucleon is treated as a genuine three-body problem. The resulting Faddeev equation in rainbow-ladder truncation has been solved only recently for the nucleon and Δ masses [16–17] and the corresponding nucleon states

The study of axial and pseudoscalar form factors in the functional approach has so far been limited to an approximation where the nucleon is treated as a bound object of a quark and a diquark that interact via quark exchange [12, 13]. The entire gluonic substructure appears here only implicitly within the dressing of quark and diquark propagators as well as diquark vertex functions. There are several conceptual issues that complicate the treatment of form factors in the quark-diquark model. First, the requirement of current conservation induces the appearance of intricate 'seagull' diagrams [14]. Such terms have been taken into account for electromagnetic form factors, but their implementation in the case of axial form factors has not yet been possible for technical reasons [13]. Second, to comply with chiral Ward identities, a current-conserving quark-diquark model requires vector diquarks in addition to the usual scalar and axialvector diquark degrees of freedom [15]. Such an elaborate treatment of the quark-diquark model has not yet been performed.

Goldberger-Treiman relation and $g_{\pi NN}$ from the three quark BS / Faddeev approach in the NJL model

Noriyoshi Ishii (Erlangen - Nuremberg U.) (Apr 28, 2000)

Published in: *Nucl.Phys.A* 689 (2001) 793-845 • e-Print: [nucl-th/0004063](https://arxiv.org/abs/nucl-th/0004063) [nucl-th]

Axial Form Factors

- Hellstern, G. and Alkofer, Reinhard and Oettel, M. and Reinhardt, H., *Nucl.Phys.A* 627 (1997) 679-709.
- Bloch, Jacques C. R. and Roberts, Craig D. and Schmidt, S. M., *Phys.Rev.C* 61 (2000) 065207.
- Oettel, Martin and Pichowsky, Mike and von Smekal, Lorenz, *Eur.Phys.J.A* 8 (2000) 251-281.
- Eichmann, G. and Fischer, C. S., *Eur.Phys.J.A* 48 (2012) 9.
- Chen Chen, C. S. Fischer, C. D. Roberts and J. Segovia (2020), Form Factors of the Nucleon Axial Current, *Phys.Lett.B* 815 (2021) 136150.
- Chen Chen, C. S. Fischer, C. D. Roberts and J. Segovia (2021), Nucleon axial-vector and pseudoscalar form factors, and PCAC relations, submitted to *Phys.Rev.D*.

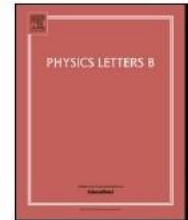
Physics Letters B 815 (2021) 136150



Contents lists available at ScienceDirect

Physics Letters B

www.elsevier.com/locate/physletb



Form factors of the nucleon axial current

Chen Chen^a, Christian S. Fischer^{a,b}, Craig D. Roberts^{c,d,*}, Jorge Segovia^{e,d}



^a Institut für Theoretische Physik, Justus-Liebig-Universität Gießen, D-35392 Gießen, Germany

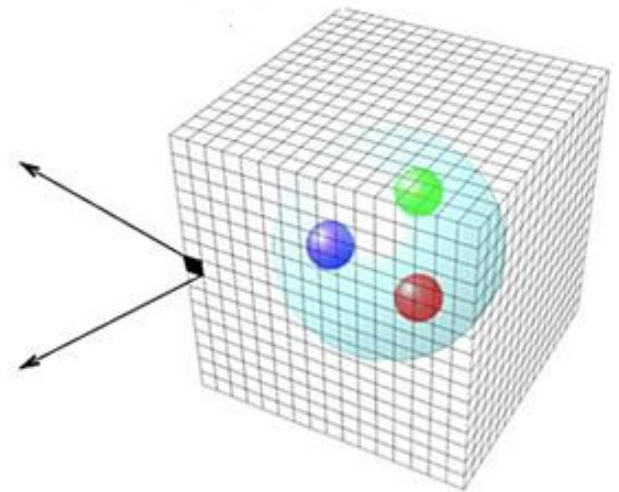
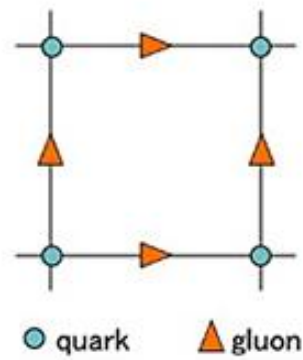
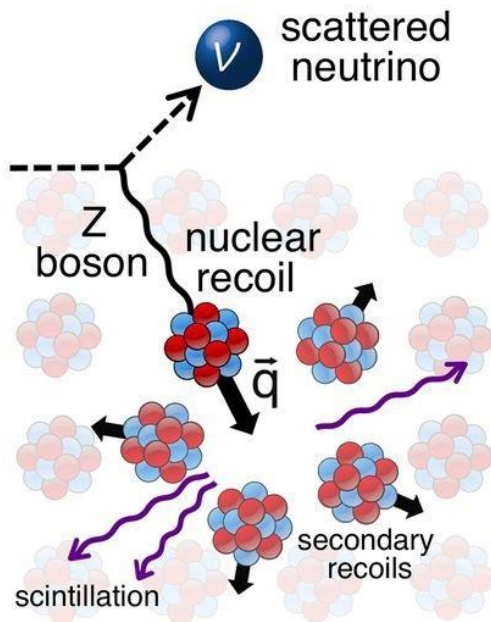
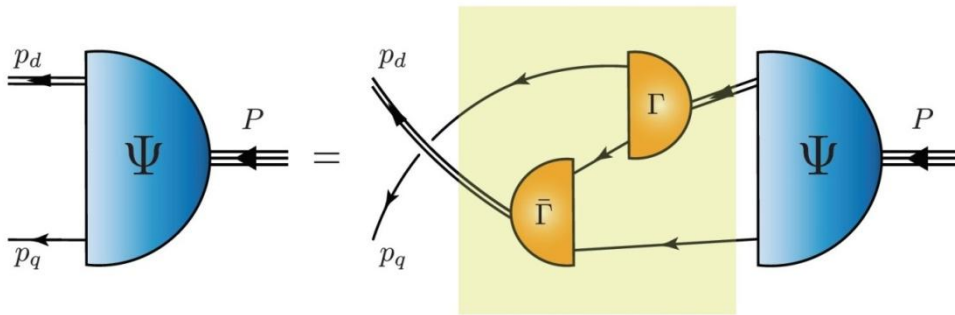
^b Helmholtz Forschungssakademie Hessen für FAIR (HFHF), GSI Helmholtzzentrum für Schwerionenforschung, Campus Gießen, 35392 Gießen, Germany

^c School of Physics, Nanjing University, Nanjing, Jiangsu 210093, China

^d Institute for Nonperturbative Physics, Nanjing University, Nanjing, Jiangsu 210093, China

^e Dpto. Sistemas Físicos, Químicos y Naturales, Univ. Pablo de Olavide, E-41013 Sevilla, Spain

Numerical Results

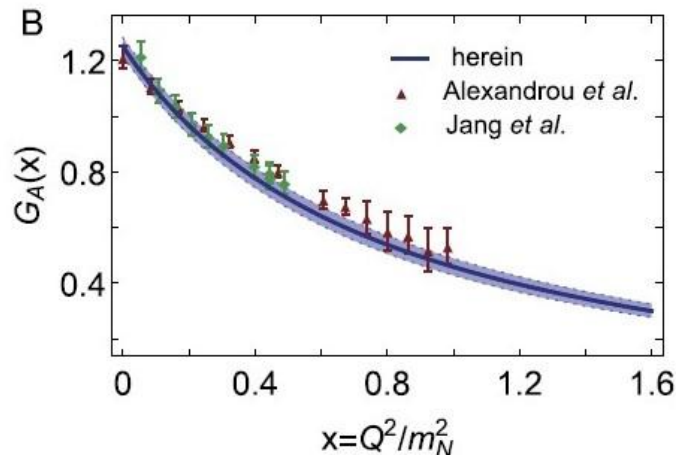
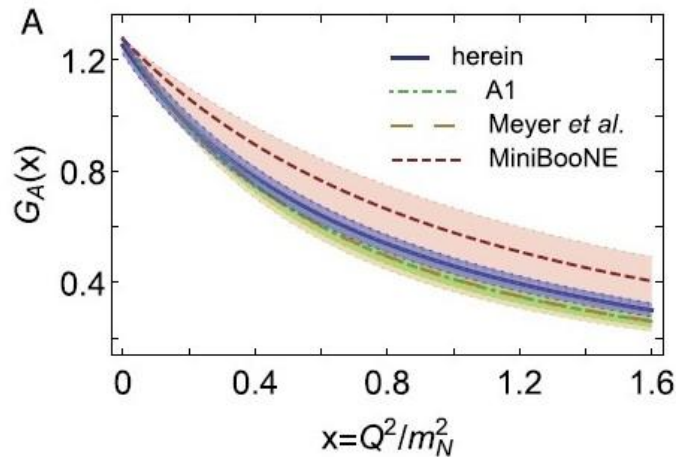


The axial current – G_A & G_P

$$J_{5\mu}^j(K, Q) = \bar{u}(P_f) \frac{\tau^j}{2} \gamma_5 \left[\gamma_\mu G_A(Q^2) + i \frac{Q_\mu}{2m_N} G_P(Q^2) \right] u(P_i)$$

➤ Two form factors:

- G_A – axial form factor



The axial current – G_A & G_P

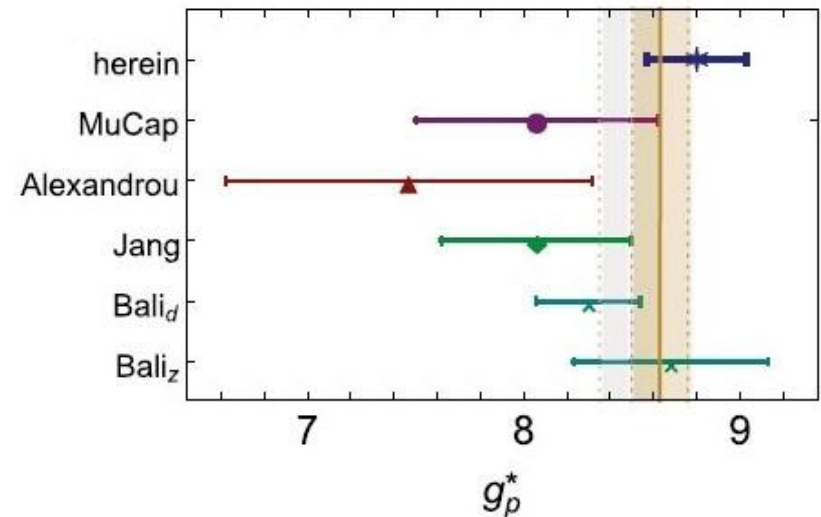
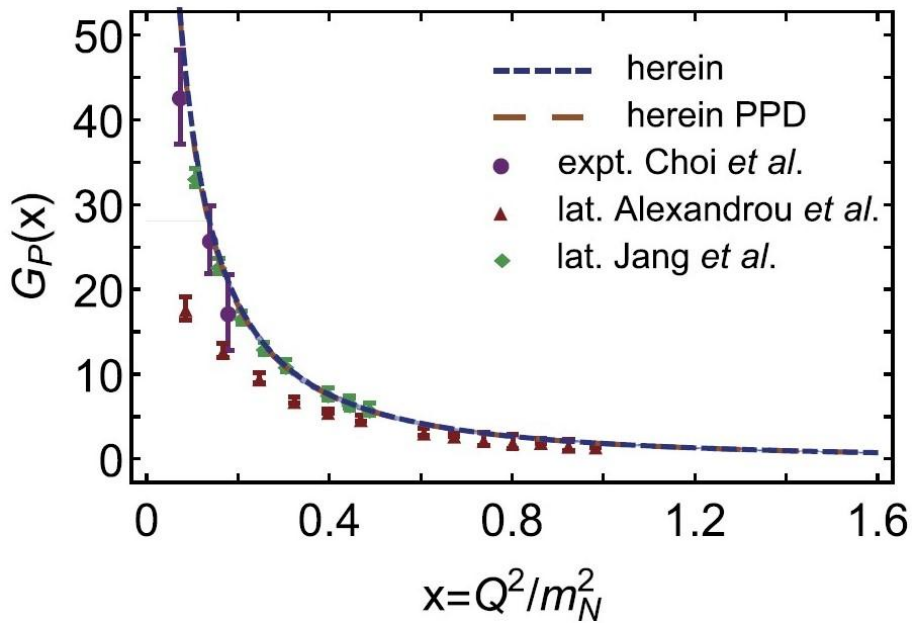
$$J_{5\mu}^j(K, Q) = \bar{u}(P_f) \frac{\tau^j}{2} \gamma_5 \left[\gamma_\mu G_A(Q^2) + i \frac{Q_\mu}{2m_N} G_P(Q^2) \right] u(P_i)$$

➤ Two form factors:

- G_A – *axial form factor*
- G_P – *induced pseudoscalar form factor*

➤ The nucleon's induced pseudoscalar charge: $g_p^* = \frac{m_\mu}{2m_N} G_P(Q^2 = 0.88m_\mu^2)$

➤ Pion pole dominance (PPD) approximation: $G_P(x) \approx \frac{4}{x + m_\pi^2/m_N^2} G_A(x)$

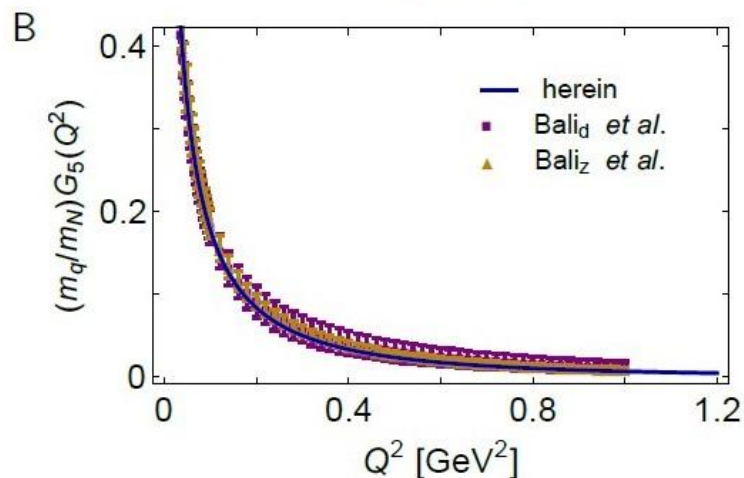
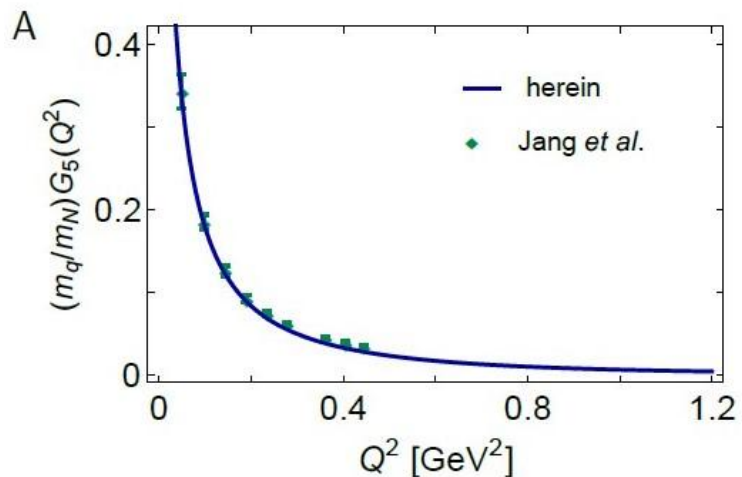


The pseudoscalar current – G_5

$$J_5^j(K, Q) = \bar{u}(P_f) \frac{\tau^j}{2} \gamma_5 G_5(Q^2) u(P_i)$$

➤ One form factor:

- G_5 – pseudoscalar form factor



The pseudoscalar current – G_5 & $G_{\pi NN}$

$$J_5^j(K, Q) = \bar{u}(P_f) \frac{\tau^j}{2} \gamma_5 G_5(Q^2) u(P_i)$$

➤ **One form factor:**

- G_5 – *pseudoscalar form factor*

➤ **At the pion mass pole, the residue of G_5 is the pion-nucleon coupling constant $g_{\pi NN}$. Thus one can define the *pion-nucleon form factor* $G_{\pi NN}$:**

$$G_5(Q^2) =: \frac{m_\pi^2}{Q^2 + m_\pi^2} \frac{f_\pi}{m_q} G_{\pi NN}(Q^2)$$

$$G_{\pi NN}(Q^2 = -m_\pi^2) = g_{\pi NN}$$

➤ **The Goldberger-Treiman relation:**

$$G_A(0) = \frac{f_\pi}{m_N} G_{\pi NN}(0)$$

➤ **The Goldberger-Treiman discrepancy (measures the distance from the chiral limit):**

$$\begin{aligned} \Delta_{GT} &= 1 - \frac{G_A(0)}{\frac{f_\pi}{m_\pi} G_{\pi NN}(-m_\pi^2)} \\ &= 1 - \frac{G_{\pi NN}(0)}{G_{\pi NN}(-m_\pi^2)} \end{aligned}$$

The pseudoscalar current – G_5 & $G_{\pi NN}$

$$J_5^j(K, Q) = \bar{u}(P_f) \frac{\tau^j}{2} \gamma_5 G_5(Q^2) u(P_i) \quad A$$

➤ **One form factor:**

- G_5 – pseudoscalar form factor

➤ **At the pion mass pole, the residue of G_5 constant $g_{\pi NN}$. Thus one can define the μ**

$$G_5(Q^2) =: \frac{m_\pi^2}{Q^2 + m_\pi^2} \frac{f_\pi}{m_q} G_{\pi NN}(Q^2)$$

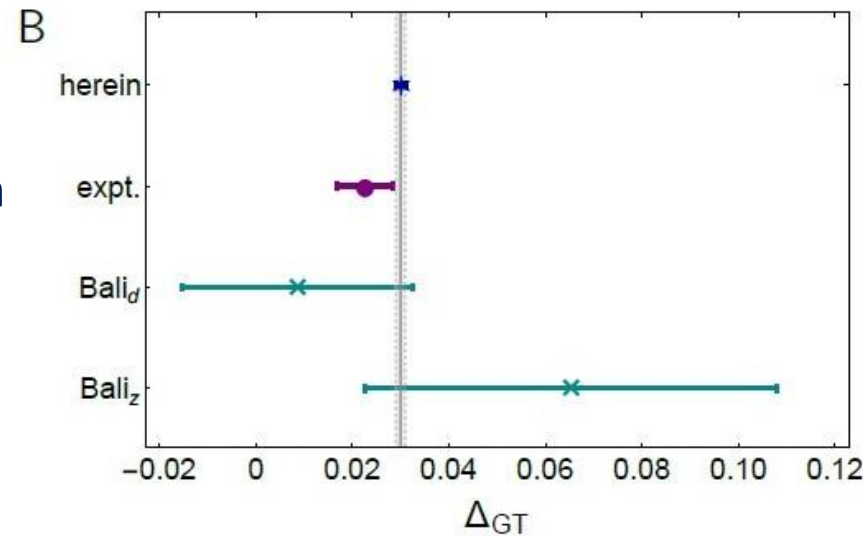
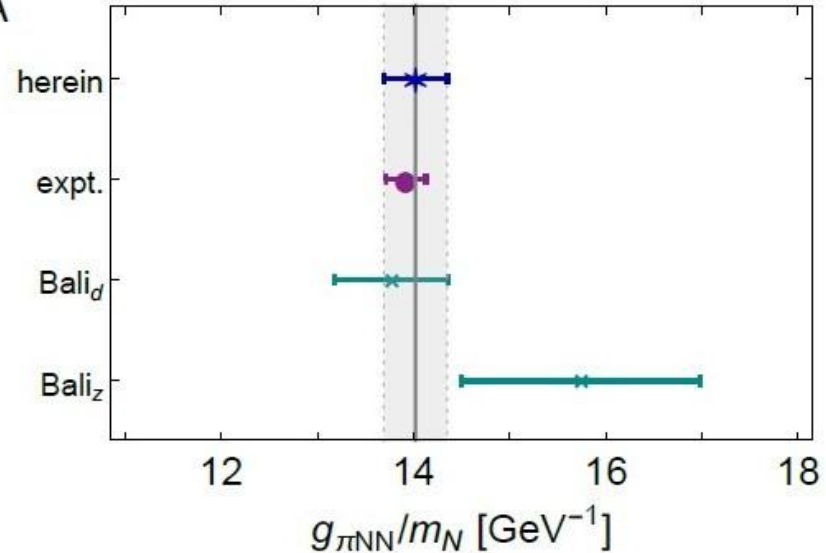
$$G_{\pi NN}(Q^2 = -m_\pi^2) = g_{\pi NN}$$

➤ **The Goldberger-Treiman relation:**

$$G_A(0) = \frac{f_\pi}{m_N} G_{\pi NN}(0)$$

➤ **The Goldberger-Treiman discrepancy (in chiral limit):**

$$\begin{aligned} \Delta_{GT} &= 1 - \frac{G_A(0)}{\frac{f_\pi}{m_\pi} G_{\pi NN}(-m_\pi^2)} \\ &= 1 - \frac{G_{\pi NN}(0)}{G_{\pi NN}(-m_\pi^2)} \end{aligned}$$



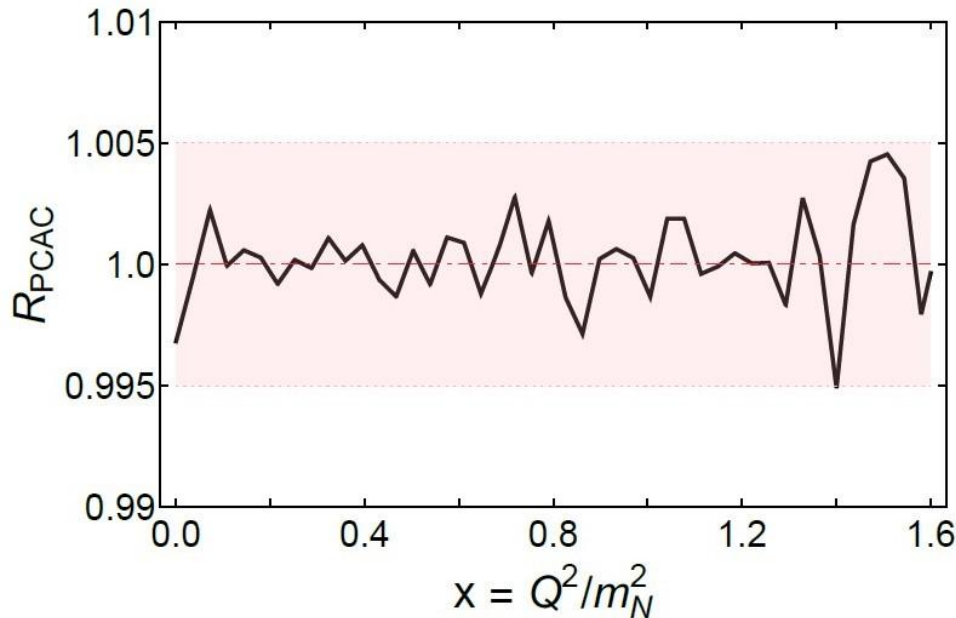
PCAC

➤ The Partially Conservation of the Axial Current (PCAC) relation:

$$G_A(Q^2) - \frac{Q^2}{4m_N^2} G_P(Q^2) = \frac{m_q}{m_N} G_5(Q^2)$$

➤ Define: the PCAC ratio

$$R_{\text{PCAC}} := \frac{4m_N^2 G_A}{Q^2 G_P + 4m_q m_N G_5}$$



D. Proof of PCAC

We have specified all the necessary building blocks to construct the diagrams of $J_{5\mu}^j(K, Q)$ and $J_5^j(K, Q)$ depicted in Fig. 3, with the corresponding expressions given in Appendix B. Before we perform numerical computations, it is important to prove analytically the PCAC relation, Eq. (7), *i.e.* $J_{5\mu}^j(K, Q)$ and $J_5^j(K, Q)$ are both a sum of six terms (listed in Fig. 3):

$$J_{5(\mu)}^j = J_{5(\mu)}^q + J_{5(\mu)}^{\text{dq},aa} + (J_{5(\mu)}^{\text{dq},sa} + J_{5(\mu)}^{\text{dq},as}) + J_{5(\mu)}^{\text{ex}} + J_{5(\mu)}^{\text{sg}} + \bar{J}_{5(\mu)}^{\text{sg}}. \quad (68)$$

Note too that, in this proof, we shall consider either the neutral (τ^3) or the charged ($\tau^{1\pm i2}$) currents; in the isospin limit, their flavor coefficients are precisely the same.

Diagram 1: current coupling to quark line

For Diagram 1 in Fig. 3, contracting Eq. (B.2) with Q_μ and using Eq. (17), we obtain³

$$Q_\mu J_{5\mu}^{q,0+}(K, Q) + 2im_q J_5^{q,0+}(K, Q) = \frac{1}{2} \int_p \bar{\Psi}^{0+}(p'_f; -P_f) S(p_{q+}) [Q_\mu \Gamma_{5\mu}(p_{q+}, p_{q-}) +$$

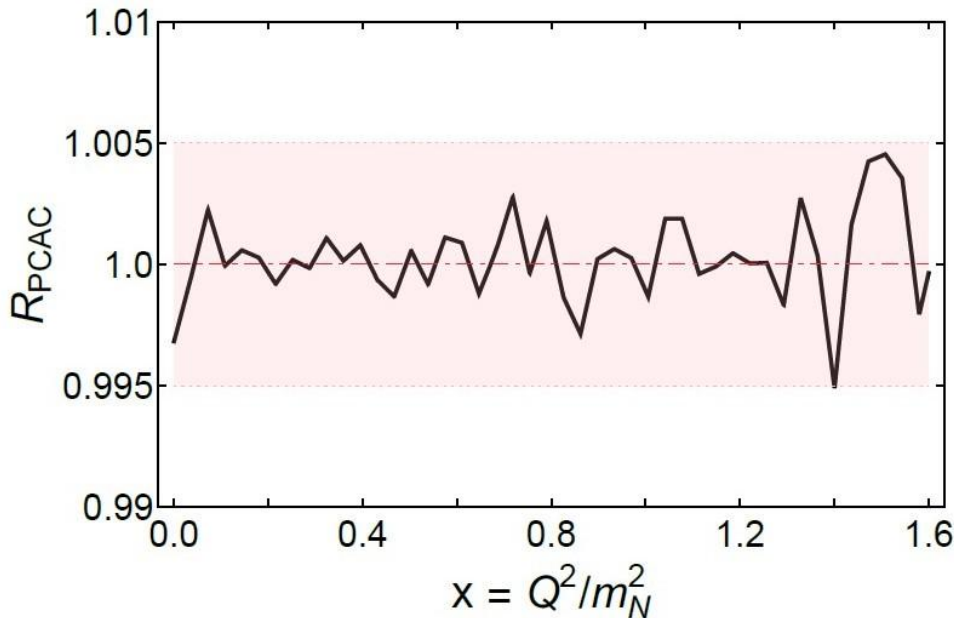
PCAC

➤ The Partially Conservation of the Axial Current (PCAC) relation:

$$G_A(Q^2) - \frac{Q^2}{4m_N^2} G_P(Q^2) = \frac{m_q}{m_N} G_5(Q^2)$$

➤ Define: the PCAC ratio

$$R_{\text{PCAC}} := \frac{4m_N^2 G_A}{Q^2 G_P + 4m_q m_N G_5}$$



$$\begin{aligned} & Q_\mu J_{5\mu}^{\bar{sg},1^+1^+} + 2im_q J_5^{\bar{sg},1^+1^+} \\ &= \int_p \int_k \bar{\Phi}_{\alpha,f}^{1^+} \left[\left(\frac{1}{12} \right) \Gamma_\beta^{1^+}(\tilde{k}_r) S^T(\tilde{q}) \bar{\Gamma}_\alpha^{1^+}(\tilde{p}_r) i\gamma_5 + \right. \\ & \quad \left. \left(-\frac{5}{12} \right) \Gamma_\beta^{1^+}(\tilde{k}_r) S^T(\tilde{q}) i\gamma_5^T \bar{\Gamma}_\alpha^{1^+}(\tilde{p}_r) \right] \Phi_{\beta,i}^{1^+}; \quad (95) \end{aligned}$$

The color/flavor coefficients in the first lines of Eqs. (92)-(95) are calculated via Eq. (C.10), *i.e.* the bystander legs of the seagulls' conjugations; and the coefficients in the second lines are calculated via Eq. (C.9), the exchange legs.

Sum of all contributions

Using Eqs. (68), (73), (78), (79), (80), (81), (86) and (91), it is straightforward to obtain their sum:

$$\begin{aligned} Q_\mu J_{5\mu}^j(K, Q) + 2im_q J_5^j(K, Q) &= \sum_{J_1^{P_1}, J_2^{P_2}=0^+, 1^+} \\ & \left[(Q_\mu J_{5\mu}^{q, J_1^{P_1} J_2^{P_2}}(K, Q) + 2im_q J_5^{q, J_1^{P_1} J_2^{P_2}}(K, Q)) \right. \\ & + (Q_\mu J_{5\mu}^{\text{ex}, J_1^{P_1} J_2^{P_2}}(K, Q) + 2im_q J_5^{\text{ex}, J_1^{P_1} J_2^{P_2}}(K, Q)) \\ & + (Q_\mu J_{5\mu}^{\text{sg}, J_1^{P_1} J_2^{P_2}}(K, Q) + 2im_q J_5^{\text{sg}, J_1^{P_1} J_2^{P_2}}(K, Q)) \\ & \left. + (Q_\mu J_{5\mu}^{\bar{sg}, J_1^{P_1} J_2^{P_2}}(K, Q) + 2im_q J_5^{\bar{sg}, J_1^{P_1} J_2^{P_2}}(K, Q)) \right] \\ &= 0, \quad (96) \end{aligned}$$

where $j = 3$ for the neutral current, or $j = 1 \pm i2^{21}$ for the charged currents.

Summary & Perspective

- Solved the seagull term problem for the axial and pseudoscalar currents, which had defied our understanding for more than **20** years.
- Computed the form factors **G_A** , **G_P** and **G_5** .
- The **PCAC** relation can be satisfied precisely.
- Next:
 - ❑ Compute the axial Delta-→Delta, N-→ Delta, N-→Roper...
 - ❑ In the three-body framework, revisiting the computation of Eichmann & Fischer (2011) first.

Thank you!

Dyson-Schwinger equations (DSEs)

Quark propagator:

$$\text{---}\bigcirc\text{---}^{-1} = \text{---}^{-1} + \text{---}\bigcirc\text{---}$$

Ghost propagator:

$$\text{---}\bigcirc\text{---}^{-1} = \text{---}^{-1} + \text{---}\bigcirc\text{---}$$

Ghost-gluon vertex:

$$\text{---}\bigcirc\text{---} = \text{---} + \text{---}\bigcirc\text{---}$$

Gluon propagator:

$$\text{---}\bigcirc\text{---}^{-1} = \text{---}^{-1} +$$

Quark-gluon vertex:

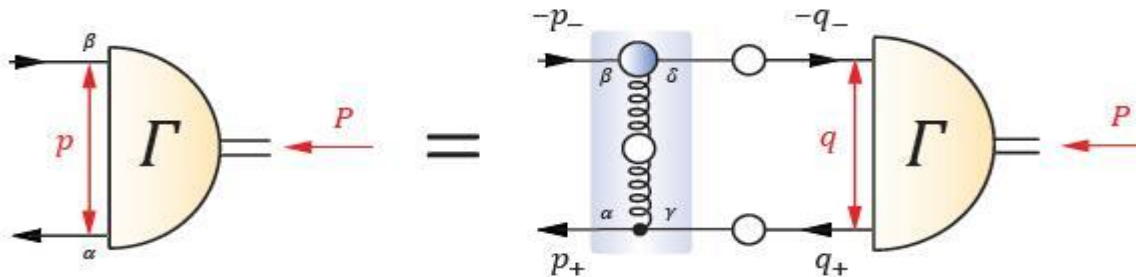
$$\text{---}\bigcirc\text{---} = \text{---} +$$

Hadrons: Bound-states in QFT

➤ **Mesons:** a 2-body bound state problem in QFT

➤ Bethe-Salpeter Equation

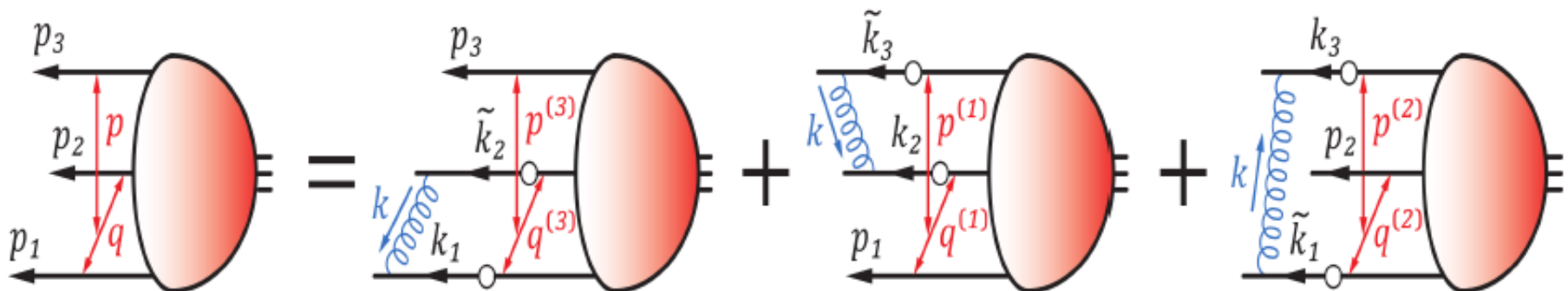
➤ **K** - fully amputated, two-particle irreducible, quark-antiquark scattering kernel



➤ **Baryons:** a 3-body bound state problem in QFT.

➤ Faddeev equation: sums all possible quantum field theoretical exchanges and interactions that can take place between the three dressed-quarks that define its valence quark content.

Faddeev equation in rainbow-ladder truncation

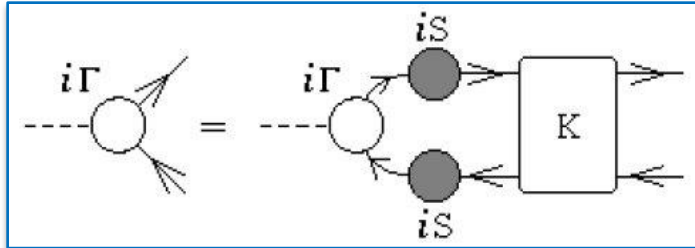


Hadrons: Bound-states in QFT

➤ **Mesons:** a 2-body bound state problem in QFT

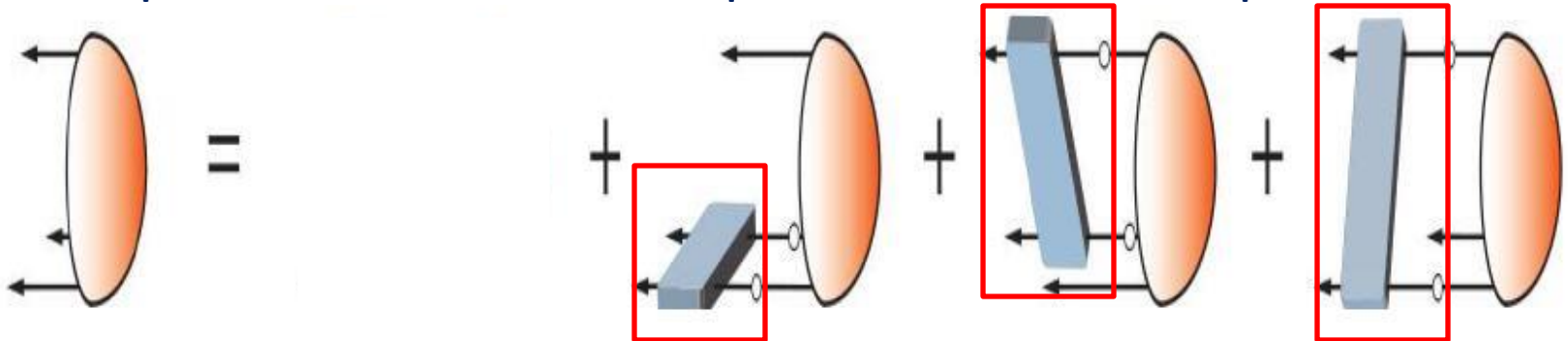
➤ Bethe-Salpeter Equation

➤ **K** - fully amputated, two-particle irreducible, quark-antiquark scattering kernel



➤ **Baryons:** a 3-body bound state problem in QFT

➤ Faddeev equation: sums all possible quantum field theoretical exchanges and interactions that can take place between the three dressed-quarks that define its valence quark content.



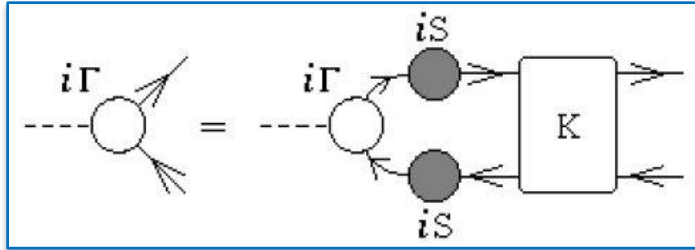
□ The **diquark Ansatz** for the 4-point Green's function of the quark-quark correlations.

Hadrons: Bound-states in QFT

➤ **Mesons:** a 2-body bound state problem in QFT

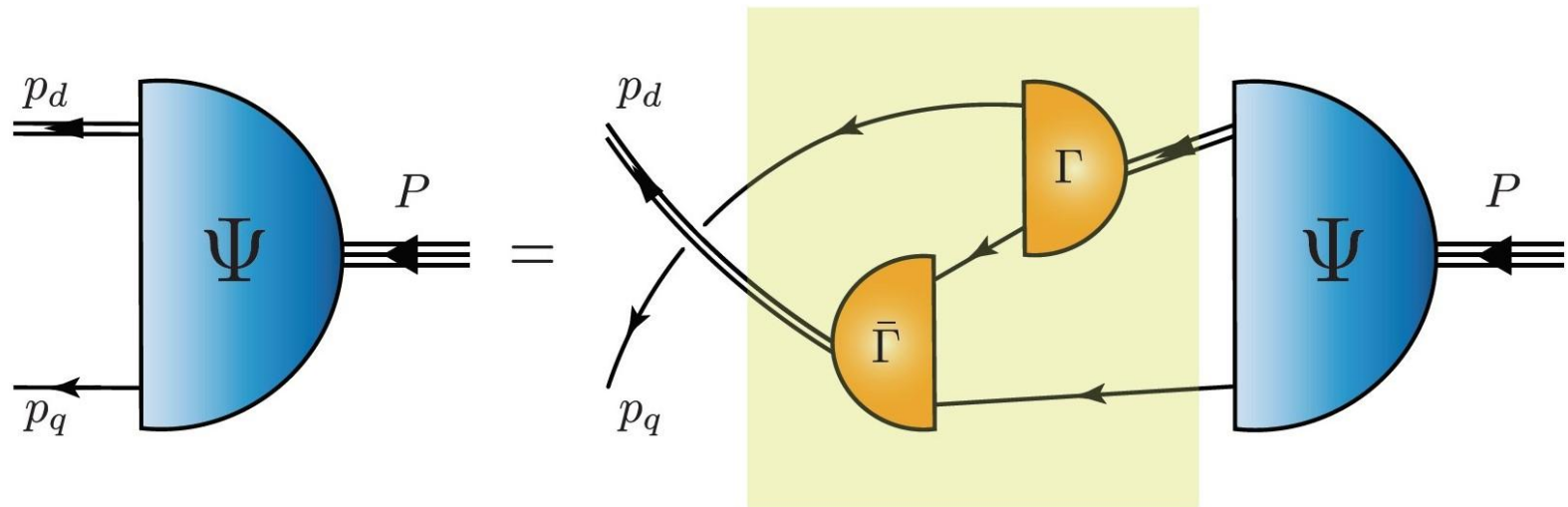
➤ Bethe-Salpeter Equation

➤ **K** - fully amputated, two-particle irreducible, quark-antiquark scattering kernel



➤ **Baryons:** a 3-body bound state problem in QFT

➤ Faddeev equation: sums all possible quantum field theoretical exchanges and interactions that can take place between the three dressed-quarks that define its valence quark content.



Building blocks (I)

➤ The current-quark vertices

- The axial-vector Ward-Takahashi identity:

$$Q_\mu \Gamma_{5\mu}^j(k_+, k_-) + 2im_q \Gamma_5^j(k_+, k_-) = S^{-1}(k_+) i\gamma_5 \frac{\tau^j}{2} + \frac{\tau^j}{2} i\gamma_5 S^{-1}(k_-)$$

- The Bethe-Salpeter Amplitude of the pion:

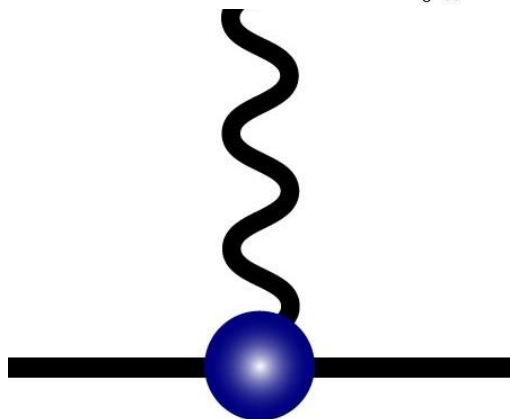
$$\Gamma_\pi^j(k, Q) = \tau^j \gamma_5 \left[i E_\pi(k, Q) \right]$$

- One Ansatz: $E_\pi(k, Q) = \frac{1}{2f_\pi} (B(k_+^2) + B(k_-^2))$

$$S^{-1}(k) = i\gamma \cdot k A(k^2) + B(k^2)$$

in the chiral limit:

$$E_\pi(k, 0) = \frac{B(k^2)}{f_\pi}$$



Therefore, we finally arrive at

$$\Gamma_{5\mu}^j(k_+, k_-) = \frac{\tau^j}{2} \gamma_5 \left[\gamma_\mu \Sigma_A(k_+^2, k_-^2) + 2\gamma \cdot k k_\mu \Delta_A(k_+^2, k_-^2) + 2i \frac{Q_\mu}{Q^2 + m_\pi^2} \Sigma_B(k_+^2, k_-^2) \right], \quad (28)$$

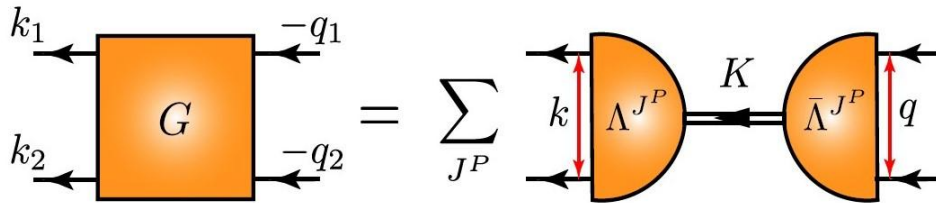
and

$$\begin{aligned} i\Gamma_5^j(k_+, k_-) &= \frac{m_\pi^2}{Q^2 + m_\pi^2} \frac{f_\pi}{2m_q} \Gamma_\pi^j(k, Q) \\ &\equiv \frac{\tau^j}{2} \frac{m_\pi^2}{Q^2 + m_\pi^2} \frac{1}{m_q} i\gamma_5 \Sigma_B(k_+^2, k_-^2), \quad (29) \end{aligned}$$

Building blocks (II)

➤ The seagull terms

- The diquark *Ansatz* for the 4-point Green's function of the quark-quark correlations:

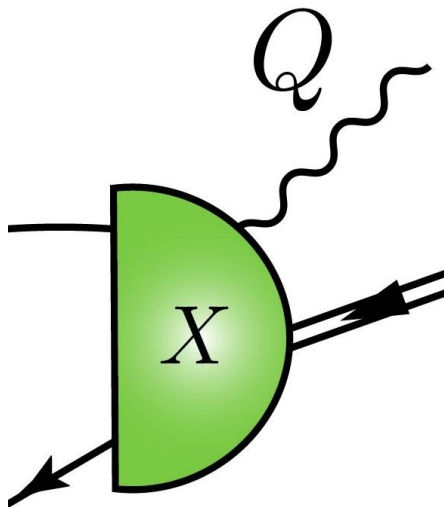


✓ Martin Oettel, Mike Pichowsky, Lorenz von Smekal, Eur.Phys.J. A8 (2000) 251-281

- The equaltime commutators of the axial current operator:

$$[\mathcal{A}_{5\mu=4}^j(x), \psi(y)]_{x_4=y_4} = \frac{\tau^j}{2} \gamma_5 \psi(x) \delta^{(4)}(x - y)$$

$$[\mathcal{A}_{5\mu=4}^j(x), \bar{\psi}(y)]_{x_4=y_4} = \bar{\psi}(x) \gamma_5 \frac{\tau^j}{2} \delta^{(4)}(x - y)$$



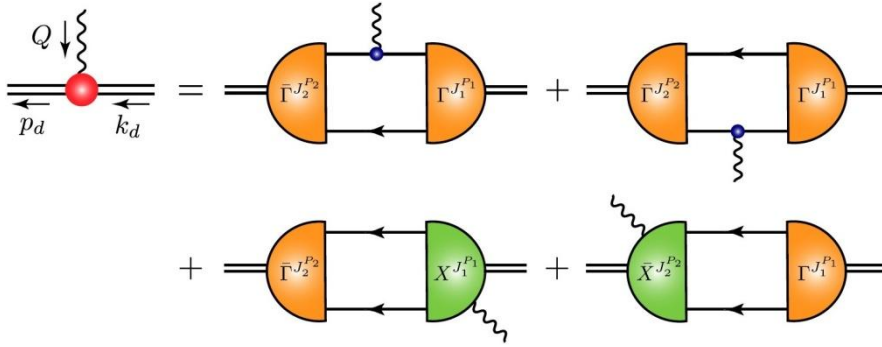
$$\chi_{5\mu, [\text{sg}]}^{j, J^P}(k, Q) = - \frac{Q_\mu}{Q^2 + m_\pi^2} \left[\frac{\tau^j}{2} i \gamma_5 \Gamma^{J^P}(k - Q/2) + \Gamma^{J^P}(k + Q/2) (i \gamma_5 \frac{\tau^j}{2})^T \right], \quad (57)$$

and

$$i \chi_{5, [\text{sg}]}^{j, J^P}(k, Q) = - \frac{1}{2m_q} \frac{m_\pi^2}{Q^2 + m_\pi^2} \left[\frac{\tau^j}{2} i \gamma_5 \Gamma^{J^P}(k - Q/2) + \Gamma^{J^P}(k + Q/2) (i \gamma_5 \frac{\tau^j}{2})^T \right]. \quad 29 \quad (58)$$

Building blocks (III)

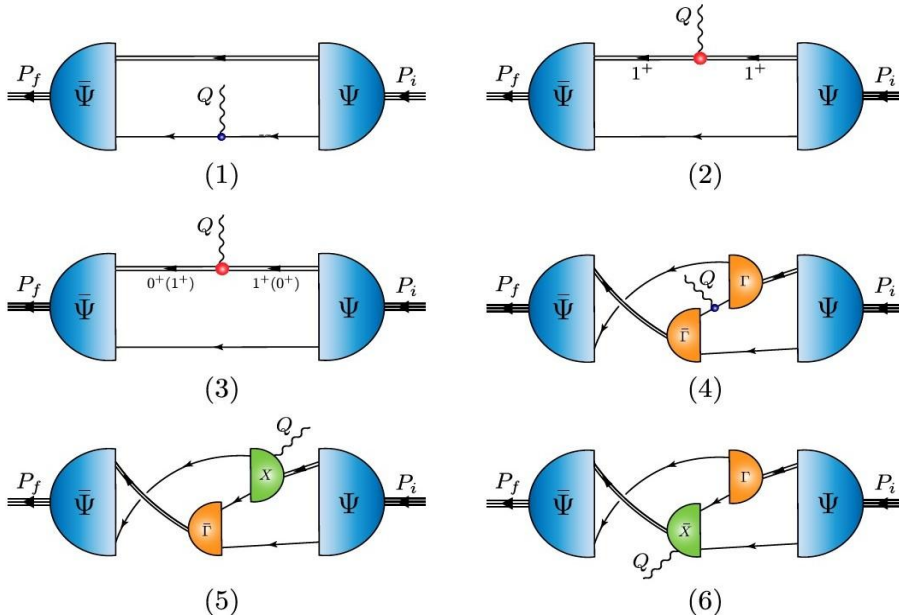
➤ The current-diquark vertices



➤ AXWTIs:

$$Q_\mu \Gamma_{5\mu,\alpha\beta}^{aa}(p_d, k_d) + 2im_q \Gamma_{5,\alpha\beta}^{aa}(p_d, k_d) = 0$$

$$Q_\mu \Gamma_{5\mu,\beta}^{sa}(p_d, k_d) + 2im_q \Gamma_{5,\beta}^{sa}(p_d, k_d) = 0$$



i) The $\{qq\}_{1+}$ -pseudoscalar-current vertex

$$\begin{aligned} \Gamma_{5,\alpha\beta}^{aa}(p_d, k_d) &= \\ &= \frac{1}{2m_q} \frac{m_\pi^2}{Q^2 + m_\pi^2} \left(\kappa_{ps}^{aa} \frac{M_q^E}{m_N} \epsilon_{\alpha\beta\gamma\delta} (p_d + k_d)_\gamma Q_\delta \right) d(\tau^{aa}), \end{aligned} \quad (61)$$

ii) The $\{qq\}_{1+}$ -axial-current vertex

$$\begin{aligned} \Gamma_{5\mu,\alpha\beta}^{aa}(p_d, k_d) &= \left(\frac{\kappa_{ax}^{aa}}{2} \epsilon_{\mu\alpha\beta\nu} (p_d + k_d)_\nu + \right. \\ &\quad \left. + \frac{Q_\mu}{Q^2 + m_\pi^2} \left(\kappa_{ps}^{aa} \frac{M_q^E}{m_N} \epsilon_{\alpha\beta\gamma\delta} (p_d + k_d)_\gamma Q_\delta \right) \right) d(\tau^{aa}), \end{aligned} \quad (62)$$

iii) The pseudoscalar-current induced $0^+ \leftarrow 1^+$ transition vertex

$$\begin{aligned} \Gamma_{5,\beta}^{sa}(p_d, k_d) &= \\ &= \frac{1}{2m_q} \frac{m_\pi^2}{Q^2 + m_\pi^2} \left(-2i\kappa_{ps}^{sa} M_q^E Q_\beta \right) d(\tau^{sa}), \end{aligned} \quad (63)$$

iv) The axial-current induced $0^+ \leftarrow 1^+$ transition vertex

$$\begin{aligned} \Gamma_{5\mu,\beta}^{sa}(p_d, k_d) &= \left(im_N \kappa_{ax}^{sa} \delta_{\mu\beta} + \right. \\ &\quad \left. + \frac{Q_\mu}{Q^2 + m_\pi^2} \left(-2i\kappa_{ps}^{sa} M_q^E Q_\beta \right) \right) d(\tau^{sa}). \end{aligned} \quad (64)$$

The axial current – G_A & G_P

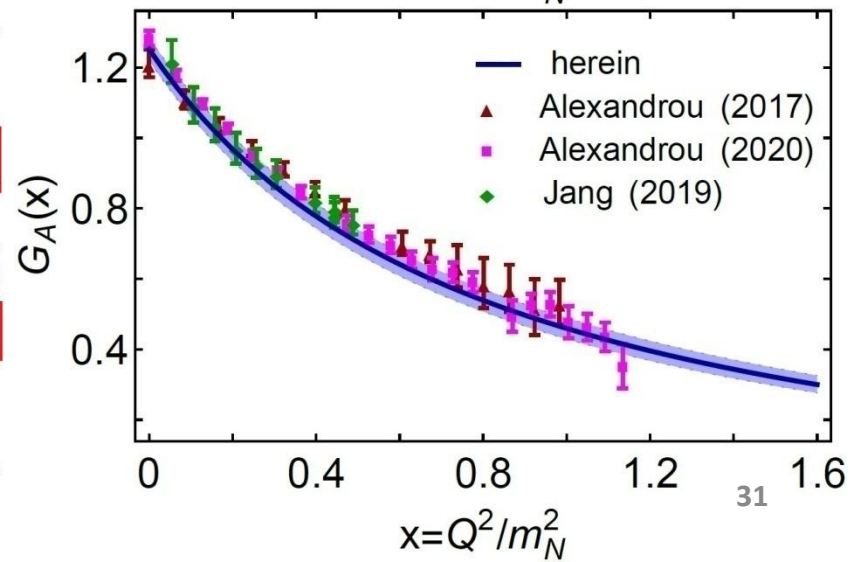
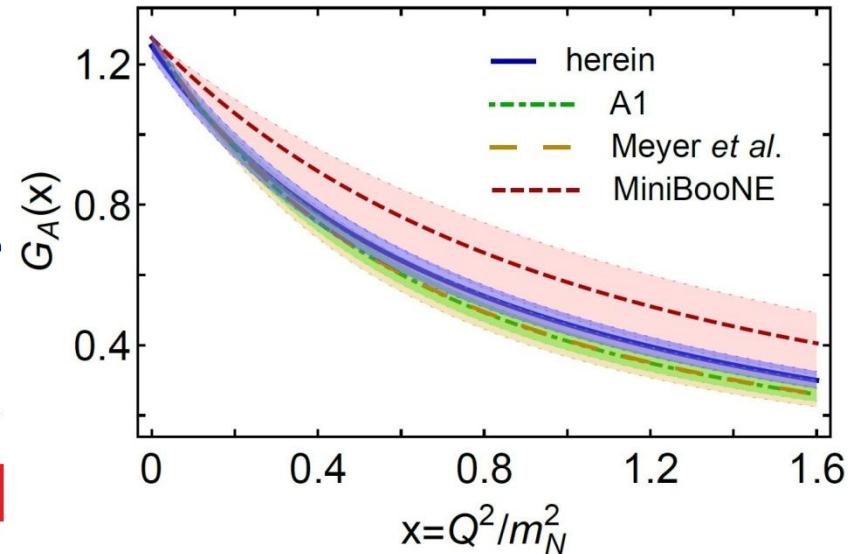
$$J_{5\mu}^j(K, Q) = \bar{u}(P_f) \frac{\tau^j}{2} \gamma_5 \left[\gamma_\mu G_A(Q^2) + i \frac{Q_\mu}{2m_N} G_P(Q^2) \right] u(P_i)$$

➤ Two form factors:

- G_A – axial form factor
- G_P – induced pseudoscalar form factor

➤ G_A can reliably be represented by dipole characterised by mass-scale m_A

	g_A	$m_N \langle r_A^2 \rangle^{1/2}$	m_A/m_N
Herein	1.25(03)	3.25(04)	1.23(03)
Faddeev ₃ [31]	0.99(02)	2.63(06)	1.32(03)
Exp [4]	1.2756(13)	–	–
Exp [13]	–	3.02(11)	1.15(04)
Exp [14]	–	3.23(72)	1.15(08)
Exp [17]	–	2.41(31)	1.44(18)
IQCD [57]	1.21(3)(2)	2.45(08)(03)	1.41(04)(02)
IQCD [58]	1.30(6)	3.57(30)	0.97(16)
IQCD _d [59]	1.23(3)	2.48(15)	1.39(09)
IQCD _z [59]	1.30(9)	3.19(30)	1.09(11)



The axial current – G_A & G_P

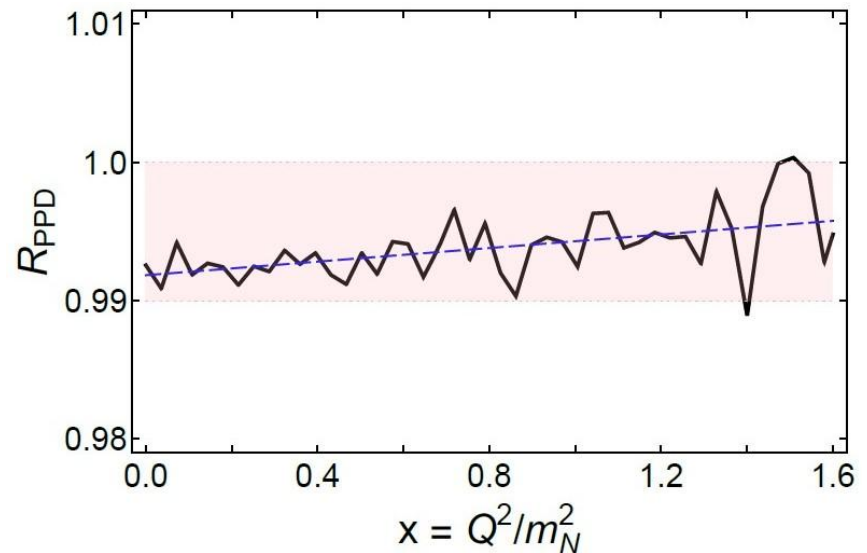
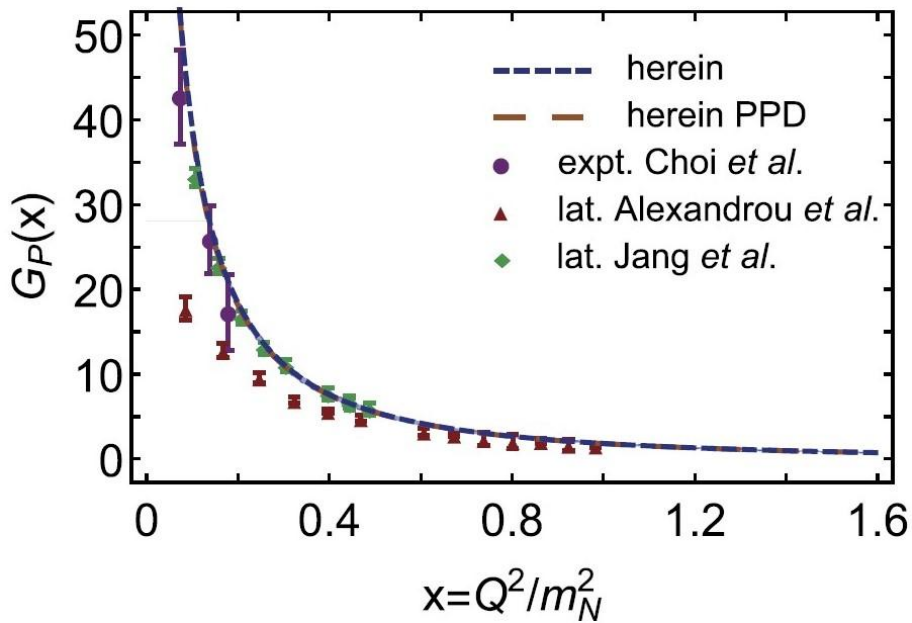
$$J_{5\mu}^j(K, Q) = \bar{u}(P_f) \frac{\tau^j}{2} \gamma_5 \left[\gamma_\mu G_A(Q^2) + i \frac{Q_\mu}{2m_N} G_P(Q^2) \right] u(P_i)$$

➤ Two form factors:

- G_A – *axial* form factor
- G_P – *induced pseudoscalar* form factor

➤ The nucleon's induced pseudoscalar charge: $g_p^* = \frac{m_\mu}{2m_N} G_P(Q^2 = 0.88m_\mu^2)$

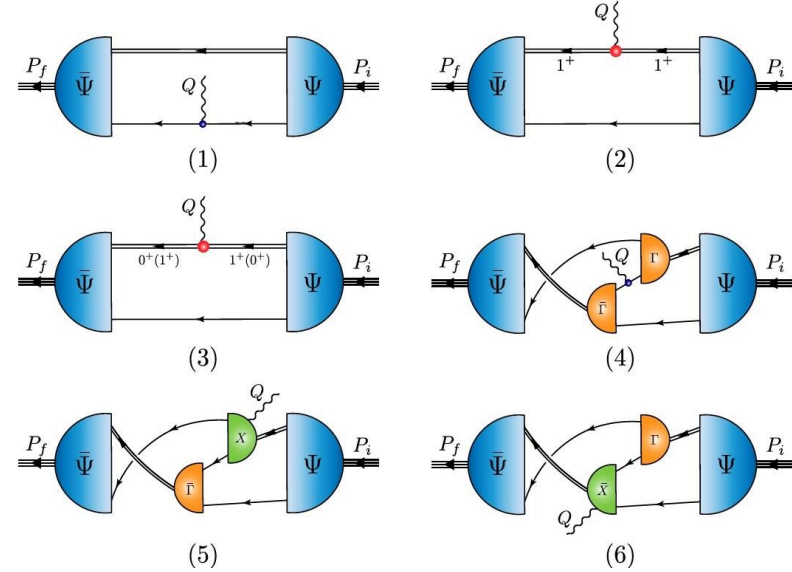
➤ Pion pole dominance (PPD) approximation: $G_P(x) \approx \frac{4}{x + m_\pi^2/m_N^2} G_A(x)$



Fractions of $G_A(0)$, $G_P(0)$ and $G_5(0)$

TABLE I. Referring to Fig. 3, separation of $G_A(0)$, $G_P(0)$ and $G_5(0)$ into contributions from various diagrams, listed as a fraction of the total $Q^2 = 0$ value. Diagram (1): $\langle J \rangle_q^S$ – weak-boson strikes dressed-quark with scalar diquark spectator; and $\langle J \rangle_q^A$ – weak-boson strikes dressed-quark with axial-vector diquark spectator. Diagram (2): $\langle J \rangle_{qq}^{AA}$ – weak-boson interacts strikes axial-vector diquark with dressed-quark spectator. Diagram (3): $\langle J \rangle_{dq}^{SA+AS}$ – weak-boson mediates transition between scalar and axial-vector diquarks, with dressed-quark spectator. Diagram (4): $\langle J \rangle_{\text{ex}}$ – weak-boson strikes dressed-quark “in-flight” between one diquark correlation and another. Diagrams (5) and (6): $\langle J \rangle_{\text{sg}}$ – weak-boson couples inside the diquark correlation amplitude. The listed uncertainty in these results reflects the impact of $\pm 5\%$ variations in the diquark masses in Eq. (16), *e.g.* $0.71_{1\mp} \Rightarrow 0.71 \mp 0.01$.

	$\langle J \rangle_q^S$	$\langle J \rangle_q^A$	$\langle J \rangle_{qq}^{AA}$	$\langle J \rangle_{dq}^{SA+AS}$	$\langle J \rangle_{\text{ex}}$	$\langle J \rangle_{\text{sg}}$
$G_A(0)$	$0.71_{4\mp}$	$0.064_{2\pm}$	$0.025_{5\pm}$	$0.13_{0\mp}$	$0.072_{32\pm}$	0
$G_P(0)$	$0.74_{4\mp}$	$0.070_{5\pm}$	$0.025_{5\pm}$	$0.13_{0\mp}$	$0.22_{4\pm}$	$-0.19_{1\mp}$
$G_5(0)$	$0.74_{4\mp}$	$0.069_{5\pm}$	$0.025_{5\pm}$	$0.13_{0\mp}$	$0.22_{4\pm}$	$-0.19_{1\mp}$



➤ Projections:

$$G_A = -\frac{1}{4(1+\tau)} \text{tr}_D [J_{5\mu} \gamma_5 \gamma_\mu^T],$$

$$G_P = \frac{1}{\tau} \left(G_A - \frac{Q_\mu}{4im_N \tau} \text{tr}_D [J_{5\mu} \gamma_5] \right),$$

$$G_5 = \frac{1}{2\tau} \text{tr}_D [J_5 \gamma_5],$$

➤ $G_P(0) \sim G_5(0)$

$$G_P \sim \frac{Q_\mu}{\tau^2} \text{tr}_D [J_{5\mu} \gamma_5] \sim \frac{1}{\tau} \text{tr}_D [J_5 \gamma_5] \sim G_5,$$

when $Q^2 \sim 0 \text{ GeV}^2$.

QCD-kindred model

➤ The dressed-quark propagator

$$S(p) = -i\gamma \cdot p \sigma_V(p^2) + \sigma_S(p^2)$$

➤ algebraic form:

$$\begin{aligned} \bar{\sigma}_S(x) = & 2\bar{m}\mathcal{F}(2(x + \bar{m}^2)) \\ & + \mathcal{F}(b_1x)\mathcal{F}(b_3x)[b_0 + b_2\mathcal{F}(\epsilon x)], \end{aligned} \quad (\text{A3a})$$

$$\bar{\sigma}_V(x) = \frac{1}{x + \bar{m}^2} [1 - \mathcal{F}(2(x + \bar{m}^2))], \quad (\text{A3b})$$

with $x = p^2/\lambda^2$, $\bar{m} = m/\lambda$,

$$\mathcal{F}(x) = \frac{1 - e^{-x}}{x}, \quad (\text{A4})$$

$\bar{\sigma}_S(x) = \lambda\sigma_S(p^2)$ and $\bar{\sigma}_V(x) = \lambda^2\sigma_V(p^2)$. The mass scale, $\lambda = 0.566$ GeV, and parameter values,

$$\begin{array}{ccccc} \bar{m} & b_0 & b_1 & b_2 & b_3 \\ \hline 0.00897 & 0.131 & 2.90 & 0.603 & 0.185 \end{array}, \quad (\text{A5})$$

associated with Eq. (A3) were fixed in a least-squares fit to light-meson observables [79,80]. [$\epsilon = 10^{-4}$ in Eq. (A3a) acts only to decouple the large- and intermediate- p^2 domains.]

QCD-kindred model

➤ The dressed-quark propagator

$$S(p) = -i\gamma \cdot p \sigma_V(p^2) + \sigma_S(p^2)$$

- Based on solutions to the gap equation that were obtained with a dressed gluon-quark vertex.
- Mass function has a real-world value at $p^2 = 0$, NOT the highly inflated value typical of **RL** truncation.
- Propagators are entire functions, consistent with sufficient condition for confinement and completely unlike known results from **RL** truncation.
- Parameters in quark propagators were fitted to a diverse array of meson observables. **ZERO** parameters changed in study of baryons.
- Compare with that computed using the DCSB-improved gap equation kernel (DB).
The parametrization is a sound representation numerical results, although simple and introduced long beforehand.

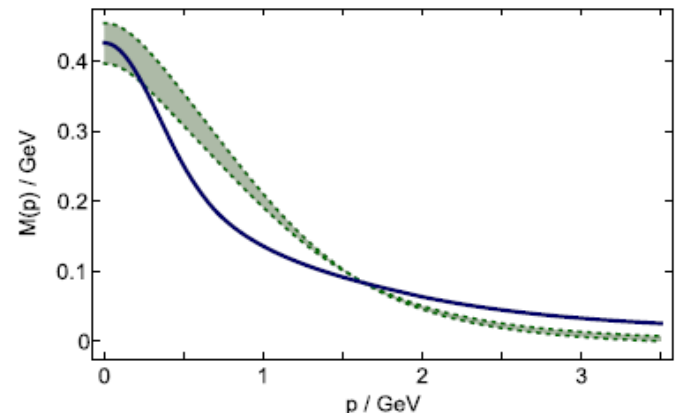


FIG. 6. Solid curve (blue)—quark mass function generated by the parametrization of the dressed-quark propagator specified by Eqs. (A3) and (A4) (A5); and band (green)—exemplary range of numerical results obtained by solving the gap equation with the modern DCSB-improved kernels described and³⁵used in Refs. [16,81–83].

QCD-kindred model

- **Diquark amplitudes:** five types of correlation are possible in a $J=1/2$ bound state: isoscalar scalar($I=0, J^P=0^+$), isovector pseudovector, isoscalar pseudoscalar, isoscalar vector, and isovector vector.
- The **LEADING** structures in the correlation amplitudes for each case are, respectively (Dirac-flavor-color),

$$\Gamma^{0+}(k; K) = g_{0+} \gamma_5 C \tau^2 \vec{H} \mathcal{F}(k^2 / \omega_{0+}^2),$$

$$\vec{\Gamma}_{\mu}^{1+}(k; K) = i g_{1+} \gamma_{\mu} C \vec{\tau} \vec{H} \mathcal{F}(k^2 / \omega_{1+}^2),$$

$$\Gamma^{0-}(k; K) = i g_{0-} C \tau^2 \vec{H} \mathcal{F}(k^2 / \omega_{0-}^2),$$

$$\Gamma_{\mu}^{1-}(k; K) = g_{1-} \gamma_{\mu} \gamma_5 C \tau^2 \vec{H} \mathcal{F}(k^2 / \omega_{1-}^2),$$

$$\vec{\Gamma}_{\mu}^{1-}(k; K) = i g_{1-} [\gamma_{\mu}, \gamma \cdot K] \gamma_5 C \vec{\tau} \vec{H} \mathcal{F}(k^2 / \omega_{1-}^2),$$

- **Simple form.** Just one parameter: diquark masses.
- **Match expectations** based on solutions of meson and diquark Bethe-Salpeter amplitudes.

➤ The diquark propagators

$$\Delta^{0\pm}(K) = \frac{1}{m_{0\pm}^2} \mathcal{F}(k^2/\omega_{0\pm}^2),$$

$$\Delta_{\mu\nu}^{1\pm}(K) = \left[\delta_{\mu\nu} + \frac{K_\mu K_\nu}{m_{1\pm}^2} \right] \frac{1}{m_{1\pm}^2} \mathcal{F}(k^2/\omega_{1\pm}^2).$$

- The ***F-functions***: Simplest possible form that is consistent with infrared and ultraviolet constraints of confinement (IR) and **1/q²** evolution (UV) of meson propagators.
- Diquarks are **confined**.
- free-particle-like at spacelike momenta
 - pole-free on the timelike axis
 - This is **NOT** true of **RL** studies. It enables us to reach arbitrarily high values of momentum transfer.

➤ The Faddeev amplitudes:

$$\begin{aligned}
 \psi^\pm(p_i, \alpha_i, \sigma_i) = & [\Gamma^{0+}(k; K)]_{\sigma_1 \sigma_2}^{\alpha_1 \alpha_2} \Delta^{0+}(K) [\varphi_{0+}^\pm(\ell; P) u(P)]_{\sigma_3}^{\alpha_3} \\
 & + [\Gamma_\mu^{1+j}] \Delta_{\mu\nu}^{1+} [\varphi_{1+\nu}^{j\pm}(\ell; P) u(P)] \\
 & + [\Gamma^{0-}] \Delta^{0-} [\varphi_{0-}^\pm(\ell; P) u(P)] \\
 & + [\Gamma_\mu^{1-}] \Delta_{\mu\nu}^{1-} [\varphi_{1-\nu}^\pm(\ell; P) u(P)], \quad (9)
 \end{aligned}$$

➤ Quark-diquark vertices:

$$\varphi_{0+}^\pm(\ell; P) = \sum_{i=1}^2 \mathcal{S}_i^\pm(\ell^2, \ell \cdot P) S^i(\ell; P) \mathcal{G}^\pm,$$

$$\varphi_{1+\nu}^{j\pm}(\ell; P) = \sum_{i=1}^6 \omega_i^{j\pm}(\ell^2, \ell \cdot P) \gamma_5 \mathcal{A}_\nu^i(\ell; P) \mathcal{G}^\pm,$$

$$\varphi_{0-}^\pm(\ell; P) = \sum_{i=1}^2 \mathcal{P}_i^\pm(\ell^2, \ell \cdot P) S^i(\ell; P) \mathcal{G}^\mp,$$

$$\varphi_{1-\nu}^\pm(\ell; P) = \sum_{i=1}^6 v_i^\pm(\ell^2, \ell \cdot P) \gamma_5 \mathcal{A}_\nu^i(\ell; P) \mathcal{G}^\mp,$$

where $\mathcal{G}^{+(-)} = \mathbf{I}_D(\gamma_5)$ and

$$S^1 = \mathbf{I}_D, \quad S^2 = i\gamma \cdot \hat{\ell} - \hat{\ell} \cdot \hat{P} \mathbf{I}_D$$

$$\mathcal{A}_\nu^1 = \gamma \cdot \ell^\perp \hat{P}_\nu, \quad \mathcal{A}_\nu^2 = -i\hat{P}_\nu \mathbf{I}_D, \quad \mathcal{A}_\nu^3 = \gamma \cdot \hat{\ell}^\perp \hat{\ell}_\nu^\perp$$

$$\mathcal{A}_\nu^4 = i\hat{\ell}_\nu^\perp \mathbf{I}_D, \quad \mathcal{A}_\nu^5 = \gamma_\nu^\perp - \mathcal{A}_\nu^3, \quad \mathcal{A}_\nu^6 = i\gamma_\nu^\perp \gamma \cdot \hat{\ell}^\perp - \mathcal{A}_\nu^4,$$

QCD-kindred model

- Both the Faddeev amplitude and wave function are Poincare covariant, i.e. they are qualitatively identical in all reference frames.
- Each of the scalar functions that appears is frame independent, but the frame chosen determines just how the elements should be combined.
- In consequence, the manner by which the dressed quarks' spin, S , and orbital angular momentum, L , add to form the total momentum J , is **frame dependent**: L , S are not independently Poincare invariant.
- The set of baryon **rest-frame** quark-diquark angular momentum identifications:

$$^2S: S^1, \mathcal{A}_v^2, (\mathcal{A}_v^3 + \mathcal{A}_v^5),$$

$$^2P: S^2, \mathcal{A}_v^1, (\mathcal{A}_v^4 + \mathcal{A}_v^6),$$

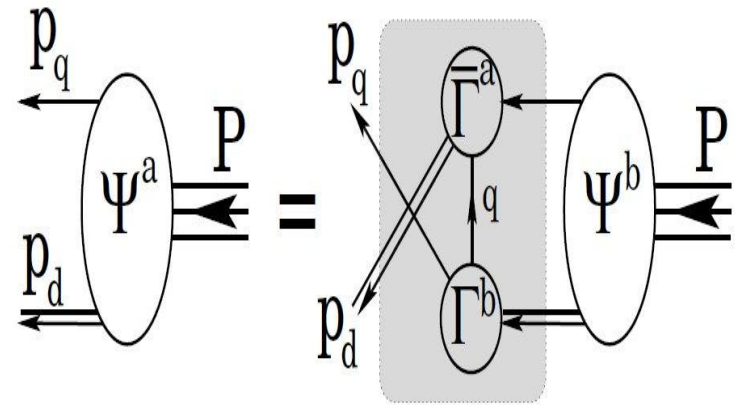
$$^4P: (2\mathcal{A}_v^4 - \mathcal{A}_v^6)/3,$$

$$^4D: (2\mathcal{A}_v^3 - \mathcal{A}_v^5)/3,$$

- The scalar functions associated with these combinations of Dirac matrices in a Faddeev wave function possess the identified angular momentum correlation between the quark and diquark.

Quark-diquark picture

- A baryon can be viewed as a Borromean bound-state, the binding within which has two contributions:
 - ✓ Formation of tight diquark correlations.
 - ✓ Quark exchange depicted in the shaded area.



- The exchange ensures that diquark correlations within the baryon are fully dynamical: no quark holds a special place.
- The rearrangement of the quarks guarantees that the baryon's wave function complies with Pauli statistics.
- Modern diquarks are different from the old static, point-like diquarks which featured in early attempts to explain the so-called missing resonance problem.
- The number of states in the spectrum of baryons obtained is similar to that found in the three-constituent quark model, just as it is in today's LQCD calculations.